



Solar Background Radiation Temperature Calibration of a Pure Rotational Raman Lidar

Vasura Jayaweera¹, Robert J. Sica¹, Giovanni Martucci², and Alexander Haeefe^{2,1}

¹Department of Physics and Astronomy, The University of Western Ontario, London, N6A 3K7, Canada

²Federal Office of Meteorology and Climatology, MeteoSwiss, CH-1530 Payerne, Switzerland

Correspondence: Alexander Haeefe (alexander.haeefe@meteoswiss.ch)

Abstract. Raman lidars are an important tool for measuring important atmospheric parameters including water vapor content and temperature in the troposphere and stratosphere. These measurements enable climatology studies and trend analyses to be performed. To detect long-term trends it is critical to have as reliable and continuous as possible calibration of the system and monitoring of its associated uncertainties. Here we demonstrate a new methodology to derive calibration coefficients for a rotational temperature Raman lidar. We use solar background measurements taken by the rotational Raman channels of the Raman Lidar for Meteorological Observations (RALMO) located at the Federal Office of Meteorology and Climatology MeteoSwiss in Payerne, Switzerland, to calculate a relative calibration as a function of time, which is made an absolute calibration by requiring only a single external calibration, in our case with a single radiosonde flight. This approach was verified using an external time series of coincident radiosonde measurements. We employed the calibration technique on historical measurements that used a Licel data acquisition system and established a calibration time series spanning from 2011 to 2015 using both the radiosonde-based external and solar background-based internal methods. Our results show that using the background calibration technique reduces the mean bias of the calibration by an average of 0.2 K across the altitude range of 1 to 16 km compared to using the local radiosoundings. Furthermore, it demonstrates the background calibration's ability to adjust and maintain continuous calibration values even amidst sudden system changes in the system, which sporadic external calibration could miss. This approach ensures that climatological averages and trends remain unaffected by the drift effects commonly associated with using daily operational radiosondes. It also allows a lidar not co-located with a routine external source to be continuously calibrated once an initial external calibration is done.

1 Introduction

Water vapor is the predominant greenhouse gas, with its abundance significantly regulated by surface temperature. When air temperature rises, the Clausius-Clapeyron equation predicts that the equilibrium vapor pressure of water will increase, leading to higher levels of water vapor in the atmosphere. Positive climate feedback, caused by an increase in water vapor concen-



tration, ultimately leads to elevated temperatures.(Colman and Soden, 2021; Dessler et al., 2013; Held and Soden, 2000). Accurate retrievals are crucial for conducting precise relative humidity climatology and trend studies in the Upper Troposphere and Lower Stratosphere (UTLS) region with Raman lidar measurements. Consequently, the credibility of the computed trends relies significantly on the reduction of uncertainties associated with these measurements. Direct retrieval of relative humidity from Raman lidar measurements necessitates the calibration of temperature measurements and a notable contributor to the uncertainty budget in Raman lidar measurements stems from these temperature calibration constants. Enhancing and refining these calibration methods are important steps toward achieving greater accuracy and reducing uncertainties in our investigations. Mahagammulla Gamage et al. (2019) proposed a method for temperature retrieval that considers the full Raman lidar equation, without requiring the assumption of an empirical calibration function. This approach mitigates uncertainties when contrasted with the utilization of empirical calibration functions, which could potentially introduce substantial errors exceeding 1 K, particularly in cases involving larger temperature ranges (Behrendt, 2005). However, it's crucial to recognize that the accuracy of this external calibration method depends on the uncertainty of the reference radiosondes. Sherlock et al. (1999) proposed an alternative approach known as the background calibration method, for calibrating water vapor mixing ratio measurements obtained through Raman backscatter water-vapor lidar systems. Their method is classified as an internal calibration technique. This method was further expanded by Hicks-Jalali et al. (2018) to generate a time series for water vapor calibration using RALMO data. This method uses the ratio of the solar background signal in detector channels to deduce a calibration constant. In this study, we will adapt this internal calibration technique to produce temperature calibration values for a rotational temperature Raman lidar. What sets this approach apart from the external method is its ability to calculate the complete calibration time series with just a single external calibration, effectively diminishing the uncertainty stemming from the reference instrument, and establishing a temperature calibration time series whose temporal evolution does not rely on the external measurements. This methodology offers the prospect of generating temperature and relative humidity trends that are free from the influences of radiosonde drifts.

2 Measurements and Methodology

2.1 Raman Lidar for Meteorological Observations (RALMO)

In order to develop our method, we used Raman lidar measurements obtained from the Raman Lidar for Meteorological Observations (RALMO). The lidar is located in Payerne, Switzerland at the facility of the Federal Office of Meteorology and Climatology MeteoSwiss (MeteoSwiss 46°48' N, 6°56' E, 492 m a.s.l.) and has been in near-continuous operation since 2009. RALMO was constructed at the École Polytechnique Fédérale de Lausanne (Diniov et al., 2013). RALMO's configuration includes a narrow field-of-view lidar receiver and a frequency-tripled Nd:YAG Q-switched laser producing an energy output of 300-400 mJ per pulse at 355 nm and at 30 Hz, and is capable of taking measurements continuously during both daytime and nighttime. RALMO uses a polychromator designed for Pure Rotational Raman (PRR) spectroscopy, allowing it to isolate Rayleigh and Mie lines, including the Cabannes line. PRR spectra from diatomic molecules like N₂ and O₂ have rotational lines spaced on both sides of the exciting wavelength (Stokes and anti-Stokes branches). Analyzing certain lines or groups of



adjacent lines enables the retrieval of vertical temperature profiles in the troposphere and lower stratosphere, as the intensity of these spectra is sensitive to temperature and wavelength (Dinoyev et al., 2010). Various validation studies have been conducted to assess the accuracy of RALMO measurements of temperature and water vapor. Brocard et al. (2013) conducted a validation study focusing on RALMO measurements of water vapor, employing collocated radiosondes. Their findings indicate that, on average, the water vapor mixing ratio closely matched radiosonde values, with differences of approximately 5 to 10% up to 8 km during nighttime and within 3% up to 3 km during daytime operations. Martucci et al. (2021) compared RALMO measurements with measurements from two reference operational radiosounding systems (ORSs) co-located alongside RALMO. Their findings demonstrate that RALMO measurements meet the stringent OSCAR (Observing Systems Capability Analysis and Review Tool) requirements for high-resolution numerical weather prediction (NWP) with an uncertainty of less than 1 K (https://space.oscar.wmo.int/requirements, accessed on 3 April 2024).

2.2 External Calibration for Temperature

Raman lidars necessitate calibration to derive accurate absolute temperature measurements. Mahagammulla Gamage et al. (2019) obtained relative humidity (RH) directly from RALMO measurements, using an external calibration method of temperature that relies on an external reference instrument, like a balloon-borne radiosonde. Following their methodology we can define a calibration constant, referred to as (C^*), as follows,

$$C^* = \frac{C_{JH}}{C_{JL}}, \quad (1)$$

where C_{JH} and C_{JL} represent the lidar constants for RALMO's digital channels, corresponding to the high quantum number (JH) and low quantum number (JL), respectively. Combining the Raman lidar equation for the backscattered PRR signal with equation 1, we find

$$C^* = \frac{\frac{N_{JH} - B_{JH}}{N_{JL} - B_{JL}}}{\frac{\sigma_{JH}}{\sigma_{JL}}}, \quad (2)$$

where N_{JH} and N_{JL} are the raw signals for the JH and JL digital channels, B_{JH} and B_{JL} the background photon counts for the JH and JL channels, and σ_{JH} and σ_{JL} denote the differential cross sections for the JH and JL digital channels. For the external method, GRAUN-certified radiosondes launched at nighttime were used. Equation 2 can in principle be evaluated at any altitude and we have omitted the range dependence for simplicity. We calculated the calibration constants by averaging over the 5 to 8 km altitude range, above the region of geometric overlap and at sufficient heights that the digital channels do not exhibit significant nonlinearities, which would affect the accuracy of the calibration constant.

2.3 Internal Calibration for Temperature: the Solar Background method

External calibration methods necessitate access to an external reference instrument. Depending on the instrument's location, these calibration opportunities can be days or weeks apart. Typically, balloon-borne radiosondes serve as the most commonly employed external reference. Calibration using radiosondes can be influenced by the flight path of the balloon, which, depending on atmospheric conditions, may experience horizontal drift and enter a different air mass compared to what the lidar



instrument samples. Such deviations in radiosonde measurements can substantially impact the precision and reliability of the calibration time series. To improve the precision and expand the applicability of external calibration methods, we adopted a technique that computes the relative calibration time series by determining the temporal evolution of the solar background ratio between the JH and JL digital channels. This approach mirrors Hicks-Jalali et al. (2018) internal calibration method for water vapor mixing ratio, which utilizes the solar background for tracking changes in the mixing calibration constant over time. What distinguishes this approach is its reliance on only one reference radiosonde measurement to construct the entire calibration time series. This method significantly reduces the uncertainties typically associated with external reference instruments, and makes the calibration time series independent from drifts associated with radiosonde measurements. The relative calibration time series $r_{solar}(t)$ is given by the equation,

$$r_{solar}(t) = \frac{B_{JH}^{solar}(t)}{B_{JL}^{solar}(t)}, \quad (3)$$

where B_{JH}^{solar} and B_{JL}^{solar} are the solar background levels detected by the JH and JL digital channels, respectively. To derive the background calibration constant (C^*), the function is normalized using external calibration and solar measurements taken at time t_0 as follows:

$$C^*(t) = C^*(t_0) \frac{r_{solar}(t)}{r_{solar}(t_0)}. \quad (4)$$

Here, $C^*(t_0)$ and $r_{solar}(t_0)$ can be determined using any point within the time series. For our solar background above 55 km, we used the ratio between the solar background from the total counts over 60 minutes from the high (JH) and low (JL) quantum number channels. At these altitudes in a raw 1-minute profile, the lidar signal will be completely due to background solar radiation and not the photons emitted by the laser. Also, we had to consider both the diurnal and seasonal solar cycles when using this solar background method, therefore we chose to only use the solar background at a time corresponding to the highest solar zenith angle on the winter solstice, which corresponds to a 70° zenith angle.

3 Results and Discussion

Figure 1 shows a comparison between the time series of the temperature calibration constants, derived through the application of the external calibration method and the solar background method. For the external method, the time series was computed for a selected number of dates spanning from the end of 2011 to the end of 2015, during which MeteoSwiss in Payerne, Switzerland, has been launching Vaisala RS92 and RS41 sondes to obtain GRUAN-certified profiles of temperature and humidity. For every 60 minutes of count data profiles, a profile-by-profile filtering method was implemented to identify and eliminate scans exhibiting significant cloud cover. This approach involved assessing the signal-to-noise ratio (SNR) of the Nitrogen (N₂) digital channel, focusing on the average SNR within the 12 to 14 km range. Profiles with an SNR below 1 were discarded. Furthermore, the calibration dataset used dates where the retained profiles, following the cloud-based filtering mechanism, constituted more than 75% of the initial number of profiles. The calibration time series was calculated through the utilization of reference radiosondes launched at nighttime. The background method calibration was performed daily using the procedure discussed

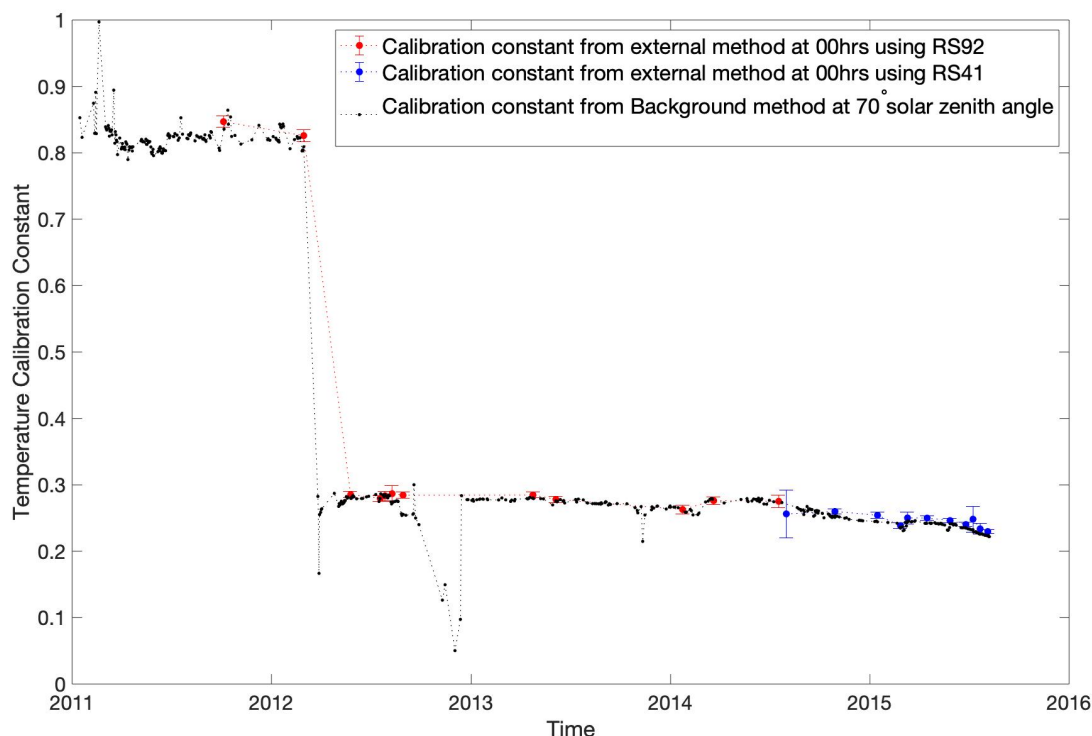


Figure 1. Comparison between the temperature calibration constant (dimensionless) obtained by the external method and the temperature calibration constant obtained using the background method. For the external method, the calibration constants were obtained using GRUAN-certified profiles of temperature from Vaisala RS92 and RS41 radiosondes launched at nighttime. For the background method, a solar background above 55 km from the high and low quantum number channels of RALMO at a time corresponding to a 70° solar zenith angle was employed. The t_0 calibration is at 2013-06-05.

above. We employed the cloud-based filtering method used in the external method to filter and discard any profiles and dates with significant cloud cover. The t_0 calibration was chosen to be 2013.06.05. This selection was made considering the error values of each external calibration constant in the time series in Figure 1, with June 5, 2013, demonstrating the lowest among all evaluated dates. We then applied the calibration technique to the measurement collected in the last 4 years of RALMO's operation using a Licel detection system. One of the prominent features of the calibration time series is the pronounced decline in the calibration constant's value seen from March to May 2012. This change is attributed to an intervention that took place to adjust one of the coaxial cables associated with the temperature polychromator component of RALMO. We can see that the notable drop observed in the external calibration time series is likewise seen in the background calibration time series, thus emphasizing the sensitivity of the background calibration method to changes within the RALMO system. This observation highlights the method's ability to measure changes in the system that could be missed with sporadic external calibration. Also,

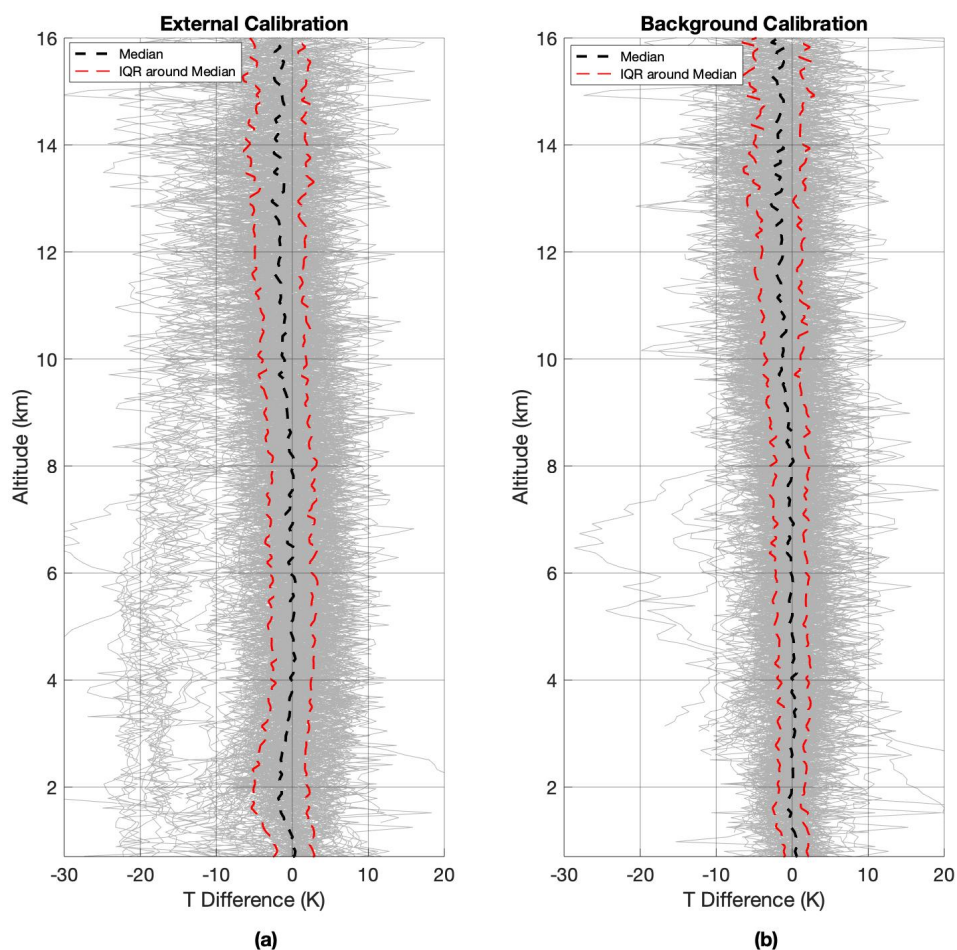


Figure 2. (a) The temperature difference between 186 OEM retrieved temperature profiles utilizing external GRAUN-sonde calibration and the homogenized radiosonde temperature profile for the years 2011 (Oct) to 2014 (Dec). (b) The temperature differential observed between 186 OEM retrieved temperature profiles utilizing the solar background calibration and the homogenized radiosonde temperature profile using measurements obtained between October 2011 and December 2014.

we can see that the calibration constant is much more stable after 2013. The agreement between the external and background methods is within a mean difference of less than 5%. Temperatures were retrieved from the lidar measurements using the OEM-based algorithm presented by Mahagammulla Gamage et al. (2019). Only digital channel measurements were used for the retrievals as the analog measurements introduced biases that we were not able to correct or explain. The OEM temperature retrieval uses the full physics of PRR scattering and can be calibrated with 1 instead of an empirical calibration function. Additionally, OEMs produce a full uncertainty budget on a profile-by-profile basis while being computationally efficient. The Licel measurements for the years 2011 to 2014 were processed, first using the calibration constants obtained using the



Table 1. Summary of the mean bias and mean IQR values across different altitude ranges for the temperature difference plots obtained using the external and the background calibration method.

Calibration Method	Mean Bias (K)				Mean IQR (K)	
	1-4 km	4-8 km	8-12 km	12-16 km	1-8 km	8-16 km
External Method	-0.9	-0.1	-1.1	-1.8	5.8	6.3
Solar Background Method	-0.02	-0.2	-1.1	-1.8	3.9	5.6

135 external method and secondly utilizing the background method. During the data processing employing external calibration coefficients, these coefficients were interpolated to align with the internal calibration points, resulting in two datasets with identical processed dates for both calibration methods. For the background calibration technique, the t_0 calibration was set on 5 June 2013, and the calibration constant $C^*(t_0)$ was computed by averaging over the 5 to 8 km altitude range. A filtering method, reliant on the cost associated with the OEM retrieval process was implemented to eliminate bad retrievals from both datasets

140 (Mahagammulla Gamage et al., 2019). Profiles with a retrieval cost lower than 0.5 or higher than 10 were discarded. Each dataset consisted of a total of 186 nights. We also used an upper-cutoff height which was determined as the altitude at which the measurement response function falls below 0.8. Below this specified altitude, the retrieval process is predominantly influenced by the measurements themselves rather than the *a priori* temperature profile. Next, we compared the 186 temperature profiles generated using the two calibration methods with those from homogenized radiosonde measurements. Note that the GRUAN-

145 certified radiosondes used for calibration are special soundings and are independent from the homogenized radiosonde data set used for validation. Figure 2a shows the temperature differences between the OEM-derived profiles utilizing the external method and correlating temperature profiles from the homogenized radiosonde data set while Figure 2b shows the comparison with the background calibration method. Table 1 summarizes the mean bias and mean Inter Quartile Range (IQR) values for the two distinct calibration methods across various altitude ranges, corresponding to the temperature difference comparison plots.

150 For the externally calibrated temperatures (Figure 2a) between 1 to 4 km, a negative mean bias of -0.9K is observed, indicating an underestimation of the lidar temperatures in this range. This negative mean bias predominantly originates from temperature retrievals obtained between February and October 2012. This period coincides with the large decline in the calibration constant time series, attributed to changes made to the RALMO system. For the subsequent altitude range of 4 to 8 km, a negative mean bias of -0.1K is observed, suggesting an underestimation in the lidar-derived temperatures within this interval. The trend

155 continues as the altitude extends to 8 to 12 km, with 12 to 16 km displaying a more substantial negative mean bias of -1.1K and -1.8K respectively, indicating a consistent tendency to underestimate temperatures in this higher altitude range.

The daily solar background-calibrated measurements have a significantly lower mean bias (0.02K) compared to those calibrated with the periodically available radiosonde calibrations in the lower altitude range of 1 to 4 km. This highlights the background calibration method's adaptability to immediately respond to changes within the RALMO system, ensuring the

160 continuity of calibration values even during abrupt system changes. This capability enables accurate retrievals, which is not feasible with the external method due to insufficient calibration points around the periods of abrupt (and unanticipated) system



changes. Between 4 to 8 km, the mean bias is -0.2K , showing a slightly higher underestimation compared to the external calibration method within this altitude span. In the subsequent 8 to 12 km and 12 to 16 km range, a mean bias of -1.1K and -1.8K is observed, an underestimation trend similar to that seen in the external calibration method.

165 For the external calibration, the IQR values over the 1 to 8 km and 8 to 16 km ranges are 5.8K and 6.3K , respectively. Meanwhile, for the background calibration, these IQR values are 3.9K and 5.6K across the same altitude intervals. These statistics show a lower variability in temperature differences when employing the background calibration, and thus, a more consistent performance over this height range compared to the external calibration method.

4 Conclusions

170 We have shown the solar background calibration method is a viable method for the temperature calibrations of rotational-Raman lidars. By using the solar background values acquired by the lidar, this technique provides a more extensive and continuous calibration timeline, which decreases the difference between the lidar and radiosonde temperatures. Notably, our study highlights the method's adaptability, showcased through its ability to swiftly adjust to modifications within the RALMO system and demonstrating its responsiveness to system variations that sporadic external calibration could miss. Moreover, the

175 solar background calibration method offers the advantage of generating a daily calibration timeline based solely on a single external reference instrument measurement which mitigates the impacts of drifts and other possible interpretation problems with comparisons to radiosondes. The solar background method is applicable to any PRR temperature lidar. The technique substantially diminishes the temperature variance relative to radiosonde calibration. The adoption of the background calibration method presents substantial benefits, especially for climatology and trend studies within the troposphere and lower stratosphere.

180 Its application ensures that climatological assessments and trend derivations remain independent of drift effects associated with radiosonde measurements.

Data availability. Measurements used in this paper may be requested from MeteoSwiss by contacting Alexander Haeefe (alexander.haeefe@meteoswiss.ch).

Author contributions. VJ was responsible for the development of the background calibration method code, generating the temperature calibration time series. VJ was also responsible for processing the RALMO data set and carrying out the validation of the calibration constants using radiosonde temperature measurements. He also wrote the initial draft of the paper. RJS wrote the underlying code for the temperature retrieval. RJS and AH defined the project scope and contributed to manuscript preparation. GM helped to validate the calibration time series by providing access to the RALMO and radiosonde measurements and provided expertise on RALMO.

185

Competing interests. The authors declare that they have no conflict of interest.



References

- Behrendt, A.: Temperature measurements with lidar, in: Lidar, pp. 273–305, Springer, 2005.
- Brocard, E., Philipona, R., Haeefe, A., Romanens, G., Mueller, A., Ruffieux, D., Simeonov, V., and Calpini, B.: Raman lidar for meteorological observations, RALMO–part 2: validation of water vapor measurements, *Atmospheric Measurement Techniques*, **6**, 1347–1358, 195 2013.
- Colman, R. and Soden, B. J.: Water vapor and lapse rate feedbacks in the climate system, *Reviews of Modern Physics*, **93**, 045 002, 2021.
- Dessler, A., Schoeberl, M., Wang, T., Davis, S., and Rosenlof, K.: Stratospheric water vapor feedback, *Proceedings of the National Academy of Sciences*, **110**, 18 087–18 091, 2013.
- Dinoev, T., Simeonov, V., Calpini, B., and Parlange, M.: Monitoring of Eyjafjallajökull ash layer evolution over payerne Switzerland with a 200 Raman lidar, *Proceedings of the TECO*, 2010.
- Dinoev, T., Simeonov, V., Arshinov, Y., Bobrovnikov, S., Ristori, P., Calpini, B., Parlange, M., and Bergh, H.: Raman lidar for meteorological observations, RALMO–Part 1: Instrument description, *Atmospheric Measurement Techniques*, **6**, 1329–1346, 2013.
- Held, I. M. and Soden, B. J.: Water vapor feedback and global warming, *Annual Review of Energy and the Environment*, **25**, 441–475, 2000.
- Hicks-Jalali, S., Sica, R., Haeefe, A., and Martucci, G.: A Calibration of the MeteoSwiss Raman Lidar for Meteorological Observations 205 (RALMO) Water Vapour Mixing Ratio Measurements using a Radiosonde Trajectory Method, in: EPJ Web of Conferences, vol. **176**, p. 08015, EDP Sciences, 2018.
- Mahagammulla Gamage, S., Sica, R. J., Martucci, G., and Haeefe, A.: Retrieval of temperature from a multiple channel pure rotational Raman backscatter lidar using an optimal estimation method, *Atmospheric Measurement Techniques*, **12**, 5801–5816, 2019.
- Martucci, G., Navas-Guzmán, F., Renaud, L., Romanens, G., Gamage, S. M., Hervo, M., Jeannet, P., and Haeefe, A.: Validation of pure rotational Raman temperature data from the Raman Lidar for Meteorological Observations (RALMO) at Payerne, *Atmospheric Measurement 210 Techniques*, **14**, 1333–1353, 2021.
- Sherlock, V., Hauchecorne, A., and Lenoble, J.: Methodology for the independent calibration of Raman backscatter water-vapor lidar systems, *Applied Optics*, **38**, 5816–5837, 1999.